Electric Power Systems Research 242 (2025) 111410

Contents lists available at ScienceDirect

Electric Power Systems Research

journal homepage: www.elsevier.com/locate/epsr

A novel predictor for areal blackout in power system under emergency state using measured data

Siavash Shadpey [a], Mohammad Reza Aghamohammadi [a,*], Alireza Sobbouhi [a], Enrico Zio [b,c]

[a] Electrical Engineering Department, Shahid Beheshti University, Tehran 19839 69411, Iran
[b] Centre de Recherche sur les Risques et les Crises (CRC), MINES Paris-PSL University, Sophia Antipolis, France
[c] Dipartimento di Energia – Politecnico di Milano, Via La Masa 34, I-20156 Milano, Italy

ARTICLE INFO

Keywords:
Areal blackout predictor
Decision tree-based ensemble algorithm
Emergency state
Moving window snapshot
Vector vulnerability index

ABSTRACT

Power systems are always under the risk of various disturbances threating their stability and integrity with the potential for blackouts. Due to unforeseen contingencies, uncertain renewable resources and insufficient corrective measures, the pre-fault dynamic security assessment (DSA) methods cannot guarantee full security under alert operating state of power systems, and pulling to emergency state becomes inevitable. Furthermore, these methods provide a global view of the security of whole power systems. To address the limitations of DSA-based methods, this paper proposes an agile approach to prevent the propagation of blackouts in the power network, requiring a local identification strategy based on blackout areas. An online power system blackout predictor (PSBP) is designed to predict the amount of future potential blackouts (AFPB) under emergency conditions as a supplement to traditional DSA methods. This approach introduces a new paradigm for system vulnerability assessment. For each blackout area, the PSBP employs decision tree-based ensemble algorithms. By continuously tracking incremental changes in the dominant transient operating variables that reflect disturbances and system vulnerability, the PSBP can predict the potential for a blackout area to progress toward a full blackout. The vulnerability index, calculated based on incremental changes observed in the moving window of snapshots (MWS), is updated incrementally. This index serves as input to the PSBP to predict the likelihood of a blackout in each area. The method is demonstrated using the IEEE 39-bus test system, and the results highlight its potential as a valuable tool for assessing the future vulnerability of power systems based on historical behavior data.

1. Introduction

1.1. Background and motivation

Power system security traditionally relays on the dynamic security assessment (DSA) which is a preventive strategy under alert state of operating environment. At each instant, power system operation could be considered in one of the four operating states, namely normal, alert, emergency and restoration [1]. The nature of DSA is preventive which under alert state uses pre-disturbance operating data to evaluate the dynamic security and identify harmful contingencies. Such DSA faces some challenges: 1-inability for covering all expected and unexpected contingencies, 2-the identified preventive measures may not be effective to guarantee power system security against critical contingencies, due to the uncertain behavior of power systems. Hence, the power systems have the potential for pulling from the alert state to the emergency state. In order to overcome the shortages of DSA, the vulnerability assessment of power systems under the emergency state using the disturbed transient operating data has been presented. In fact, post-disturbance vulnerability assessment introduces a new paradigm which acts as a supplementary for DSA. On the other hand, vulnerability assessment methods identify the vulnerability in power systems on a global scale, while adopting appropriate corrective measures requires a specific knowledge about the appropriate time and location of the blackouts at the local scale. In fact, identifying potential blackouts on an areal scale by dividing a power system into different blackout areas (BA) allows for an agile strategy under emergency state for implementing effective

* Corresponding author.
E-mail addresses: s_shadpey@sbu.ac.ir (S. Shadpey), m_aghamohammadi@sbu.ac.ir (M.R. Aghamohammadi), A_Sobbouhi@sbu.ac.ir (A. Sobbouhi), enrico.zio@polimi.it (E. Zio).

https://doi.org/10.1016/j.epsr.2025.111410
Received 12 November 2024; Received in revised form 1 January 2025; Accepted 5 January 2025
Available online 23 January 2025

Acronyms

AFPB	Amount of Future Potential Blackout
AVR	Automatic Voltage Regulator
BA	Blackout Area
BAC	Balanced Accuracy
BT	Blackout Trajectory
CDDI	Combined Distance-Distortion Index
CFSM	Cascading Failures Simulation Module
CNN	Convolutional Neural Network
DDI	Distance-Distortion Index
DT	Decision Tree
TOV	Transient Operating Variable
SSOV	Steady State Operating Variable
DTOV	Dominant Transient Operating Variable
DSA	Dynamic Security Assessment
ELM	Extreme Learning Machine
FFNN	Feed-Forward Neural Network
HC	Hierarchical Clustering
LSTM	Long-Short Term Memory
MI	Mutual Information
MLP	Multi-Layer Perceptron
MRMR	Minimal-Redundancy-Maximal-Relevance
MWS	Moving Window Snapshot
OAC	Overall Accuracy
OC	Overcurrent
OS	Out-Of-Step
PC	Pearson Correlation
PMUs	Phasor Measurement Units
PNN	Probabilistic Neural Network
PSBP	Power System Blackout Predictor
PSBT	Power System Behavioral Trajectory
RTL	Reliable Transfer Learning
RVFL	Random Vector Functional Link
SEN	Sensitivity
SP	Specificity
SPS	Special Protection Scheme
STDV	Spatial-Temporal Dynamic Visualization
STVS	Short-Term Voltage Stability
SVM	Support Vector Machine
TF	True/False
TMW	Total Moving Window of Snapshot
TSA	Transient Stability Assessment
UFLS	Under Frequency Load Shedding
VVI	Vector Vulnerability Index
WAMS	Wide Area Monitoring System

Symbols

dd	General function for DDI
k	Index type
P(x)	Marginal probability distribution
P(y)	Marginal probability distribution
P(x,y)	Joint probability distribution
d_k	Distance-distortion of vector (k)
V_r	Reference vector
NV	Number of variables of DTOV
V_k	Variable vector of interest
$\overline{V}$	The average of variable vector
PD_i^1	Initial load at bus i
PD_j^1	Initial generation at bus j
α and β	The uncertain coefficients
n	The number of blackout area
ε	Threshold value
Nb	Number of blackout area

corrective emergency actions. The literature of the online DSA and vulnerability assessment methods using pre-fault and post-fault operating data under alert and emergency states are reviewed in Section 1.2.

1.2. Literature review

In [2], Feed-forward neural network (FFNN) and graph natural network (GNN) is used for evaluating the risk of cascading failures of power systems using data mining method, in which the risk of cascading failures for various operating points of power systems under two general states as safe and unsafe are investigated. [3] presents a reliable transfer learning (RTL) method for improving DSA performance in the presence of potentially related unknown faults with incomplete data and individual decision discrepancy. The RTL method extracts the dominant-invariant class-separable features for transient stability assessment. [4] develops an ensemble representation learning scheme (ERLS) to assess data loss tolerant online short-term voltage stability as stable or unstable. This method handles missing data and derives base algorithms by spatial-temporal graph convolutional network to enhance the DSA performance. [5] presents a convolutional neural network (CNN) to assess transient voltage vulnerability as stable or unstable whose training data are prepared by the image-form sample construction (IFSC) method. Weakness in transient voltage is identified by a vulnerability index (VI). [6] uses an intelligent predictor based on support vector machine (SVM) algorithm, to identify critical lines in power systems with the potential of cascading failures. Using mutual information and entropy between operating variables, the dominant variables are extracted. For each line an individual SVM is designed. [7] proposes a data-driven scheme based on a supervised algorithm called spares projection oblique randomer forests (SPORF) for online DSA (stable/unstable), which includes offline training by critical features based on a minimal-redundancy-maximal-relevance (MRMR) criterion. The class imbalance problem is mitigated by adaptive synthetic (ADASYN) oversampling method. [8] proposes a DSA method based on multiple label learning with a training database for complete and incomplete/unseen coverage label scenarios. It considers correlation between different faults and the security assessment provides secure and insecure states of power systems. [9] proposes a unified transfer learning method for DSA for predicting transient stability of power systems with respect to eight specific fault types, in which, the knowledge learned from a task is re-used to boost performance on a related task. The proposed DSA has a good accuracy for known and unknown faults, with complete and incomplete input data. [10] provides a deep learning method for DSA based on stacked de-noising auto-encoder (SDAE) using ensemble SVMs with boosting learning method. The mutual information theory is used to delete the irrelevant features. The proposed model classifies the power system status as secure and insecure for a fixed topology in terms of transient stability. [11] proposes a data-driven approach based on random bits forest and spatial-temporal dynamic visualization (STDV) to handle the DSA for transient stability (stable/unstable) under missing data conditions. The key features are selected by bagging nearest-neighbor prediction independence test (BNNPIT) and Pearson correlation (PC). [12] presents a method based on two-stage Bayesian learning for preventive and online control of power system dynamic security. At the first stage, Bayesian deep learning is applied for learning the Probabilistic neural network (PNN) model to evaluate transient stability, and at the second stage a security-constrained optimal power flow is solved by Bayesian optimization method for dynamic security evaluation module based on Bayesian neural network. Transient stability is predicted only for six

specific fault types with a fixed topology. [13] suggests an intelligent data-based method, free from the problem of missing data, using a generative adversarial network (GAN) to evaluate dynamic security of power systems. This network consists of an extreme learning machine (ELM) and random vector functional link (RVFL) networks in order to obtain diverse results. This method is a binary classifier for evaluating transient stability for 10 faults without giving information about unstable generators. [14] proposes a robust white-box model as a decision tree (DT)-based ensemble method to maintain online PMU-based DSA model accuracy against incomplete PMU data due to PMU failure and communication loss. Only the DTs for observable grid regions remain valid to provide DSA results, and the final DSA decision is made through weighted voting from the valid DTs. Transient stability is predicted only for three specific fault types with a fixed topology. [15] presents a data-based model for training DSA in which a RVFL and ELM learning-based DSA model is trained for one fault data. Then, the model is used to identify an unknown different fault based on transfer learning theory through minimizing the difference between the trained data and unknown data. This DSA classifies transient stability as stable or unstable, considering only 8 specific fault types with fixed topology. [16] presents an online DSA model based on RVFL and ELM ensemble learning to deal with the missing data due to PMU lost events which are restored by some estimators. The DSA classifies transient stability as secure and insecure with respect to only 10 specific fault types with a fixed topology.

All the above mentioned works deal with the pre-disturbance security with respect to specific number of contingencies and fixed network configuration which are inherent shortage of DSA.

[17] introduces an online detection method for cascading failures in power systems with renewable generation based on a long-short term memory (LSTM) neural network trained on measured data. This method accounts for the uncertainties of renewable generation, loading and initial contingencies of power systems. It classifies the vulnerability of power systems in the form of potential cascading failures and non-cascading failures. [18] provides a real-time transient stability predictor for power systems based on processing the post fault signals obtained from the phasor measurement units (PMUs), using multi-layer perceptron (MLP)neural network and decision tree. [19] Presents a deep learning - based binary classifier for assessing short-term voltage stability (STVS) by using post-fault dynamic trajectories of power systems. First, a semi-supervised cluster algorithm determines the class labels of the STVS and, then, a LSTM determines the states of dynamic stability/instability of the power system. This method needs fault detection information. [20] uses a data-based method using random matrix theory to evaluate the vulnerability of power systems with big data and complex structures for voltage stability. Critical buses and dynamic response of power systems are identified without the need to the network topology. [21] introduces an online transient stability estimator which classifies three classes as stable, aperiodic unstable and oscillatory unstable using post-fault bus voltage phasor in the form of a short-term time window as well as using a CNN. This method depends on fault detection without giving any information about unstable generators. [22] provides a spatial-temporal adaptive transient stability assessment to handle the missing data due to PMU failure. The spatial-temporal information is utilized adaptively by an optimal clusters searching model based on temporal feature importance, and by constructing an ensemble mechanism of LSTM for optimal PMU clusters estimates vulnerability in term of stable and unstable states. [23] designs an ensemble DT predictor consisting of three DT for early prediction of the out-of-step state of unstable generators at the post-fault conditions. This predictor is independent of fault information, and detect occurrence, clearance and instability of fault as one task. [24] predicts the amounts of potential blackouts at the emergency state of power systems with the help of a three-stage DT-based predictor. The vulnerability indices are evaluated using post-disturbance operating variables through a moving data window, which is used as the input for the proposed predictor. [25] suggests a missing-data tolerant method for post-fault STVS assessment to handle the missed data due to PMU loss and topology changes. The vulnerability is assessed only as stable and unstable status. [26] proposes a SVM classifier to predict the vulnerability state at the post-disturbance with respect to transient stability, short-term voltage stability and short-term frequency stability. This method uses a database and dynamic vulnerability area for training the classifier, but it suffers from dependency on the fault clearing time, assessment classification only as vulnerable or invulnerable status, without no information about the amounts of blackouts. [27] covers the possibility of large-scale blackouts in European countries, examines how to avoid such blackouts, and focuses on a fast and reliable restoration strategy based on path search algorithm for selecting the best start -up generator and the tie-line succession for each phase of a restoration strategy. [28] suggests a restoration method to make the distribution system resilience better after broad blackouts in European countries, using distributed generations (DGs) for the restoration of maximum important loads. The DGs with good black start ability, load weighting, and topological importance are taken into account. In [29], for security assessment of HVDC transmission system, based on the sign of the function values of the transient energy variation at the DC transmission line a new method and a protection relay algorithm for fault detection and classification is presented.

1.3. Contributions

This paper proposes a paradigm shift in vulnerability assessment, where the future behavior of a power system towards blackouts under emergency conditions is predicted based on its current and historical performance. The causal relationship between the dynamic behavior of power systems and the occurrence of blackouts serves as the foundation for this innovative approach. This approach serves as a supplementary tool to compensate for the limitations of traditional DSA methods in preventing blackouts. To enhance prediction accuracy and practical applicability, historical behavior and system characteristics are analyzed to identify several blackout-prone areas within the power system. For each identified area, a dedicated predictor is designed. A notable feature of the proposed method is the construction of sophisticated vulnerability indices derived from raw operational data. These indices are network-size independent and effectively capture the trend of system vulnerability. The robustness and simplicity of the proposed method against missing data and broad noise are confirmed without relying on data substitution, model observability, or PMU observability, but solely on dominant transient operating variables (DTOV) and their corresponding vector vulnerability indices (VVI). The main attributes and advantages of the proposed method are as follows:

- Vulnerability/blackout is evaluated by three classes (low, moderate and critical blackouts).
- The information of fault occurrence, relays operation and controllers are not needed.
- Each blackout area uses its individual dominant transient operating variables.

The main contributions of this paper are as follows:

- Identification of blackout area in power system based on the historical behavior of load buses during emergency conditions.
- Introduction a new paradigm shift in vulnerability assessment, where the future behavior of a power system towards blackouts under emergency conditions is predicted based on its current and historical behavior.
- Introduction of sophisticated vulnerability indices derived from historical raw operational data which are network-size independent and effectively capture the trend of system vulnerability.

- The vector vulnerability indices are constructed in such way that noisy or missing data have little impact on the accuracy of the blackout predictor.

Table 1 shows a quick comparison between various techniques for evaluating the power system security and vulnerability based on their main attributes and contributions.

2. Framework of the proposed power system blackout predictor (PSBP)

The framework of the proposed PSBP is presented in Fig. 1. At the offline design stage, the PSBP is trained by simulation results of several disturbance scenarios and the evolution of DTOVs. At the online application stage, in each BA, the PMU-based wide area monitoring system (WAMS) collects DTOVs, as high-dimensional raw data reflecting the dynamic behavior of the power system in the form of a moving window snapshot (MWS) from DTOVs(t-)n-1() to DTOVs(t). These variables include the magnitude and phase angle of bus voltages, the magnitude of bus frequencies and the current flows of lines, under real-time normal or emergency transient state. Twelve distance-distortion indices (DDIs) are introduced for processing each DTOV with respect to a normal reference snapshot from which the VVI are extracted. Deviations and distortions in the power system's behavioral trend over time are captured by VVIs. These indices exhibit significant changes during a major initial disturbance and subsequent cascading failures, potentially leading to a blackout. VVIs form the input of PSBP for predicting the amount of future potential blackout (AFPB) in advance (e.g. 5 s) in each BA. The trained predictor is then used online to predict the amount of blackout under emergency state for activating corrective measures or areal special protection schemes (SPS).

In control centers, two types of defense plans are implemented to address remedial action against critical contingencies and disturbances: preventive remedial actions and corrective emergency actions. While current security strategies primarily focus on preventive actions, less attention is given to developing advanced emergency strategy measures. The proposed approach introduces a new paradigm for managing emergency conditions in control centers. Its processes and algorithms can be seamlessly integrated since the required operational data are already available through PMU and WAMS. By predicting potential future blackouts, the system can effectively trigger pre-installed corrective emergency actions [27].

2.1. Basis for blackout area identification

Knowing the location and time of blackouts in power systems is necessary to take appropriate emergency corrective measures at the right place and right time to prevent the spread of blackouts. For example, if a blackout occurs in the northern zone of a power system and no disturbance in the southern zone, appropriate corrective measures should be implemented only in the northern zone. Improper and misplaced implementation of corrective measures is ineffective in preventing blackouts propagation. On-time identification of blackout in power systems requires an agile strategy based on BAs. Establishment of BAs is based on the concept of simultaneous isolation of loads in an area. BAs could be identified using several blackout simulation results through the following steps.

1. 1-The number of times (scenario) that each of the loads is isolated separately after a disturbance is obtained.
2. 2-The number of times (scenarios) that each pair of loads (i, j) is isolated after a disturbance within a certain time interval (15 seconds based on the biggest time delay related to protective relays) is obtained.

If load i and j are isolated sequentially over a time of 15 seconds due the same disturbance in the process of cascading failure, the isolation of two loads is considered as the simultaneous isolation with high correlation.

To obtain a suitable measure for identifying simultaneous pair

Table 1
Comparative techniques for evaluating the power system security and vulnerability.

Paper	Dynamic moving window under emergency state	Areal vulnerability/blackout	Multi-level classification (More than 2 classes)	Missing data	Noisy data
[2]-2023	-	-	-	-	-
[3]-2024	-	-	-	+	-
[4]-2024	-	-	-	+	-
[5]-2024	-	-	-	-	-
[6]-2022	-	-	-	-	-
[7]-2022	-	-	-	+	+
[8]-2023	-	-	-	+	-
[9]-2021	-	-	-	+	-
[10]-2021	-	-	-	-	+
[11]-2021	-	-	-	+	-
[12]-2020	-	-	-	-	-
[13]-2019	-	-	-	+	+
[14]-2019	-	-	-	+	-
[15]-2020	-	-	-	-	-
[16]-2019	-	-	-	+	-
[17]-2023	-	-	-	+	+
[18]-2021	+	-	-	+	+
[19]-2021	-	-	-	-	-
[20]-2020	+	-	-	-	+
[21]-2020	-	-	+	+	+
[22]-2020	-	-	-	+	+
[23]-2018	+	-	-	-	+
[24]-2018	+	-	+	-	-
[25]-2018	-	-	-	+	-
[26]-2015	-	-	-	-	-
[27]-2022	+	-	-	-	-
[28]-2023	+	-	-	-	-
[29]-2024	+	-	+	-	-
Proposed method	+	+	+	+	+

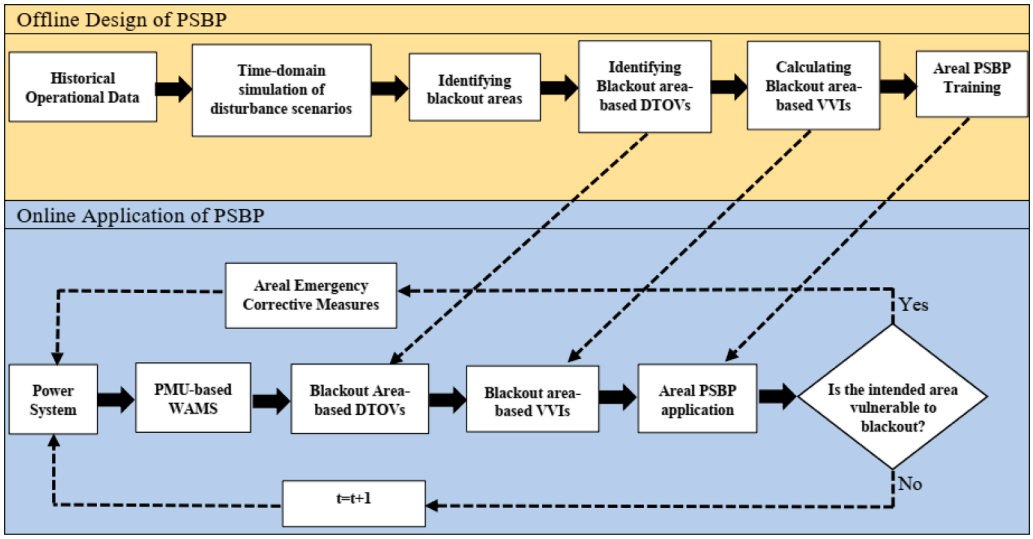

Fig. 1. Framework of the Proposed PSBP.

isolation for all combination of two loads (i, j), a measure called Jaccard is used. The probability of simultaneous pair isolation of two loads (i,j) can be calculated using Eq. (1), where, C_{ij} is the number of times/scenarios that the pair (i, j) are isolated simultaneously and NL_i and NL_j are the number of times/scenarios that loads i and j are isolated respectively within all scenarios. The closer the value of the Jaccard measure is to 1, the more correlation there is between the loads in simultaneous pair isolation, and vice versa:

$$Jaccard_{ij} = \frac{Cij}{NLi + NLj - Cij} \tag{1}$$

The values of the Jaccard measure for all pair combinations of loads are ranked from the largest to the smallest values and then the following procedure to identify the BAs in the power system is followed:

1. If each pair of loads (i, j) have not been yet assigned to any area, they form a new BA.
2. If two loads have been already assigned to two separate areas, no change is applied.
3. If load i has been previously assigned to a BA and load j has not been yet assigned to any BA, and their Jaccard value is greater than a threshold value, then the load j will belong to the area of load i. For each area, the value of the threshold is set to 50% of the value of the initial pair assigned to the area.

The process continues until all loads are assigned to the BAs.

2.2. Dominant transient operating variables in blackout areas

After identifying the BAs of a power system, it is important to identify DTOV associated to each BA. The operating variables with highest effect on the isolation of the loads in each BA constitute DTOV for that area. For identifying the corresponding DTOV to each BA, it is necessary to find the system element data (lines and buses) with the highest effect on the load isolation of the BA. For recognizing the relationship of line and bus removal with isolation of the loads in each BA, it is necessary to find their correlation based on the historical behavior of the power system. In other words, the operating variables of lines and buses whose removal has historically dominant effect on the isolation of loads in a BA constitute DTOV of that area. Regarding each scenario, for each line or bus (i) in the whole power system and load (j) in BA, there are four situations as follows:

1-Line/bus i and load j are both connected to the network, (line/bus, load) = (0,0).

2-Line/bus i is connected to the network, but load j is isolated from the network, (line/bus, load) = (0,1).

In this situation, removal of the line/bus has no effect on the isolation of the load with zero correlation.

3-Line/bus i is removed from the network, but load j is connected to the network, (line/bus, load) = (1 0).

4-Line/bus i is removed from the network and load j is isolated from the network, (line/bus, load) = (1,1).

In order to obtain the effect of the line/bus i removal on the isolation of the load j in a power system, regarding all scenarios, a probabilistic measure called Jaccard measure is used as follows [30]:

$$Jaccard_{ij} = \frac{N_{11}}{N_{11} + N_{10}} \tag{2}$$

Where, N11 and N10 are the number of situation (1,1) and (1,0) respectively within all scenarios.

$Jaccard_{ij}$ index has a value between 0, 1. The closer the value of the $Jaccard_{ij}$ index is to 1, the greater the effect of line/bus (i) removal on the isolation of load (j). If the value of $Jaccard_{ij}$ for line/bus i with respect to load j is greater than a threshold value, the line/bus i has dominant effect on isolation of load j and their operating variables (e.g. I, V, θ, f) are included in the DTOV of the BA.

2.3. Power system behavioral trajectory (PSBT)

Associated to each BA, for each respective operating snapshot at instant (t) of the real-time operation of the power system, there is a vector of DTOV(t) representative of either steady state operating variables (SSOVs) or transient operating variables (TOVs). When there is no disturbance and no significant changes, DTOV remains in normal state, and if significant changes occur it is under emergency state.

The time sequence of past snapshots over time up to instant t, including consecutive DTOVs(t) constitutes a trajectory which is defined as power system behavioral trajectory (PSBT), which updates and expands continuously. As a power system continues to operate under normal state without any disturbance, the trend of changes in PSBT is not significant. When a disturbance and subsequent cascading failures occur in the power system, the system will go under emergency state with significant changes in trend of PSBT, indicating a potential blackout amount in each BA. It is easy to understand the direct and strong relationship between the data of the PSBT and the amount of future potential blackout (AFPB) in the blackout trajectory (BT) at any given future instant (t+Δt) based on the dynamic characteristics of the

power system. In other words, the trend of PSBT can predict the potential blackout value in the future. The number of past snapshots indicates the length of the data within PSBT. Since the very past data of the PSBT have very little correlation with AFPB(t+Δt), so a certain number of past snapshots until instant t, as moving window of snapshots (MWS (t)) is taken as representative of PSBT. This length should not be too long or too short. Fig. 2 shows the trend of PSBT and BT with corresponding DTOVs within a MWS(t).

2.4. Vector vulnerability indices (VVIs)

Each vector of DTOVs in the time domain is compared with a reference vector in order to measure the trend of changes of DTOVs. For this purpose, in each BA, the distance and distortion of each vector of DTOVs is calculated relative to the reference vector and known as the distance-distortion index (DDI). According to Table 2, 12 types of distance-distortion indices are calculated [30–36] for each DTOV(j) at snapshot (j), using Eq. (3).

$$DDI_k(j) = dd_k\left(DTOV(j) - DTOV_{ref}\right) \quad \forall j = 1, \ldots, ns \quad \forall k = 1, \ldots, 12 \tag{3}$$

where dd is the general function for DDI, and k is the index type. The measured data of DTOVs within a MWS constitute a matrix MWS (NV×ns), where NV is number of variables and ns is number of snapshots.

Where dk is the distance-distortion of vector (k) with respect to reference vector (r) and $\overline{V}$ is the average.

The matrix MWS is raw data and depends on the size of the power system, it is transformed into a distance-distortion index matrix, DDI (12×ns), whose size does not depend on the size of the power system. The distance and distortion between two consecutive DTOVs within MWS (t) are measured by matrix DDI which is used as rich data for the AFPB prediction. The structure of the DDI (12×ns) matrix is presented in Fig. 3, where each column corresponds to a snapshot at instant (t) including 12 types of DDIs.

Within the matrix of DDI(12×ns) with a certain length, the beginning and the final DDIs(t) have a weaker and stronger correlation with AFPB (t+Δt), respectively because they have relatively past and present information. With respect to each type (k) of DDI, the vector of DDI_k with ns elements can be transformed into a unique number denoted as combined DDI(t) (CDDI(t)) defined by Eq. (4). This transformation reduces the amount of calculations required for the proposed predictor.

$$CDDI_k(t) = \sum_{i=1}^{ns} 2^{i-1} \times DDI_k(i) \quad \forall k = 1, \ldots, 12 \tag{4}$$

MWS(NV×ns) depends on both the size of system and number of snapshots, DDI(12×ns) depends on the number of snapshots, while CDDI is independent of both the size of system and number of snapshots. Since there are 4 types of DTOV including bus voltage magnitude, bus voltage phase angle, bus frequency and line current magnitude signals, there are 4 types of CDDI(t) totally 4×12=48 CDDIs.

For each BA, its PSBP can classify the future behavior of the BA in different levels or classes of potential blackouts based on their respective CDDIs. The most discriminating CDDI among the 48 CDDIs constitutes the vector vulnerability index (VVI) as input to PSBP. Fig. 4 shows the flow chart of data processing.

2.5. Mutual information between CDDI and AFPB

In order to find the most discriminating CDDI among the 48 CDDIs for constructing VVI as input for PSBP, the mutual information (MI) based on entropy between CDDIs and AFPB is calculated by Eq. (5) and used as criterion [37].

$$MI(CDDI,\ AFPB) = \sum\sum p(CDDI,\ AFPB)\log\left[\frac{p(CDDI,\ AFPB)}{p(CDDI).p(AFPB)}\right] \tag{5}$$

Where, *P(CDDI, AFPB)* is the joint probability distribution of CDDI and AFPB, *P(CDDI)* and *P(AFPB)* are marginal probability distribution of CDDI and AFPB respectively. The values of MI are between zero and one, indicating the minimum and maximum dependency between CDDI(t) and AFPB(t+Δt). CDDIs with corresponding MI greater than a threshold value are selected as dominant CDDIs constructing VVI.

3. The structure of the PSBP

The proposed predictor PSBP is a combination of ensemble DTs which can identify the corresponding blackout with the associated AFPB (t+Δt) in each BA for any given VVI(t) in different classes. The functional relationship between VVI(t) and AFPB(t+Δt) is shown by Fig. 5. For classifying blackout into different levels, hierarchical clustering (HC) algorithm is used to divide all VVIs(t) into different classes based on their Ward distances [38]. After classification, by grouping AFPB corresponding to all VVIs(t) belonging to each class, the level of blackout can be classified in terms of loss of MW or percentage of power loss.

Ensemble DTs algorithms are robust prediction models that combine the predictions of individual DTs to provide a more accurate prediction. Discriminating input variables accurately, reducing the risk of overfitting, and using the strengths of individual DTs are the most interesting features of the ensemble DTs. Two main and popular types of ensemble DTs are bagging and boosting using homogeneous base models [39]. In the bagging method, DTs are trained independently in parallel and combined with an averaging process. In the boosting method, DTs are trained sequentially in which each DT depends on its previous DT and their outputs are combined for final output. The bagging method has less variance than its base models, but the boosting method has less bias than its base models [39]. The structure of PSBP consisting of ensemble DTs depends on the number of classes. For example, for a system with 3

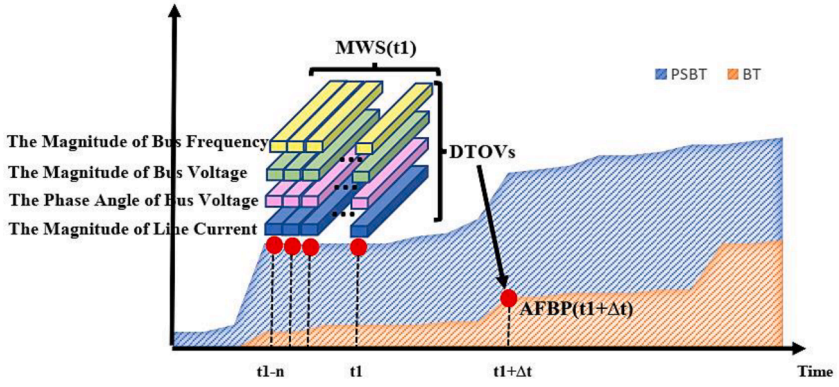

Fig. 2. Trend of PSBT and BT with DTOVs within a MWS(t).

Table 2
12 Types of DDIs.

Name	Equation	Name	Equation
DDI1.Minkowski	$d_k = \sqrt[p]{\sum_{i=1}^{n} \lvert V_{ki} - V_{ri} \rvert^p}$	DDI7. Cosine	$d_k = 1 - \frac{\sum_{i=1}^{n} V_{ki} V_{ri}}{\sqrt{\sum_{i=1}^{n} (V_{ki})^2} * \sqrt{\sum_{i=1}^{n} (V_{ri})^2}}$
DDI2. Euclidean	$d_k = \sqrt[2]{\sum_{i=1}^{n} \lvert V_{ki} - V_{ri} \rvert^2}$	DDI8. Soergel	$d_k = \frac{\sum_{i=1}^{n} \lvert V_{ki} - V_{ri} \rvert}{\sum_{i=1}^{n} max\,(V_{ki}, V_{ri})}$
DDI3. Manhattan	$d_k = \sum_{i=1}^{n} \lvert V_{ki} - V_{ri} \rvert$	DDI9. Kulczynski	$d_k = \frac{\sum_{i=1}^{n} \lvert V_{ki} - V_{ri} \rvert}{\sum_{i=1}^{n} min\,(V_{ki}, V_{ri})}$
DDI4. Sorensen	$d_k = \frac{\sum_{i=1}^{n} \lvert V_{ki} - V_{ri} \rvert}{\sum_{i=1}^{n} \lvert V_{ki} + V_{ri} \rvert}$	DDI10. Lorentzian	$d_k = \sum_{i=1}^{n} Ln(1 + \lvert V_{ki} - V_{ri} \rvert)$
DDI5. Jaccard	$d_k = \frac{\sum_{i=1}^{n} (V_{ki} - V_{ri})^2}{\sum_{i=1}^{n} (V_{ki})^2 + \sum_{i=1}^{n} (V_{ri})^2 - \sum_{i=1}^{n} V_{ki} V_{ri}}$	DDI11. Anderberg	$d_k = \frac{2(\sum_{i=1}^{n} (V_{ki} - V_{ri})^2)}{\sum_{i=1}^{n} V_{ki} V_{ri} + 2(\sum_{i=1}^{n} (V_{ki} - V_{ri})^2)}$
DDI6. Dice	$d_k = \frac{\sum_{i=1}^{n} (V_{ki} - V_{ri})^2}{\sum_{i=1}^{n} (V_{ki})^2 + \sum_{i=1}^{n} (V_{ri})^2}$	DDI12. Correlation	$d_k = 1 - \frac{\sum_{i=1}^{n} (V_{ki} - \overline{V}_k)(V_{ri} - \overline{V}_r)}{\sqrt{\sum_{i=1}^{n} (V_{ki} - \overline{V}_k)^2} \sqrt{\sum_{i=1}^{n} (V_{ri} - \overline{V}_r)^2}}$

DDI(12×ns)=

Snapshot_1	Snapshot_2	.	.	.	Snapshot_(ns-1)	Snapshot_(ns)
12DDI(t-ns+1)	*12DDI(t-ns+2)*	.	.	.	*12DDI(t-1)*	*12DDI(t)*

Fig. 3. Matrix structure of areal DDIs-based MWS(t).

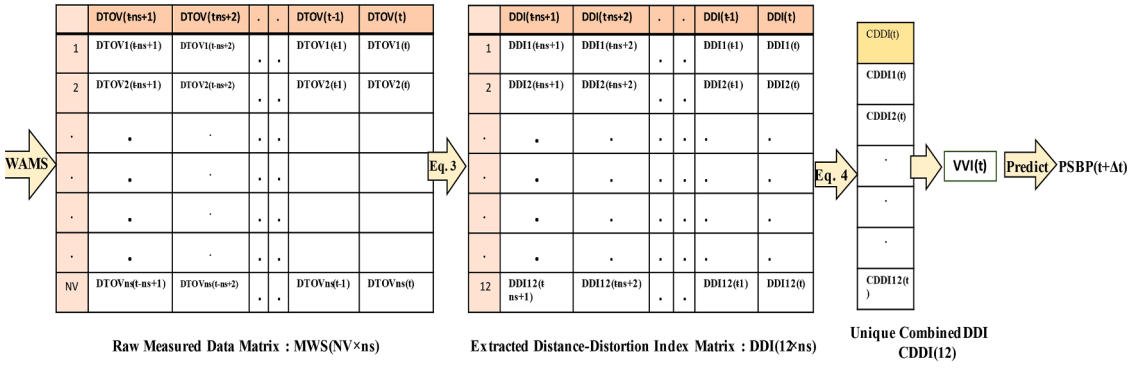

Fig. 4. Flowchart of data processing from measured raw data until vector vulnerability indices VVI.

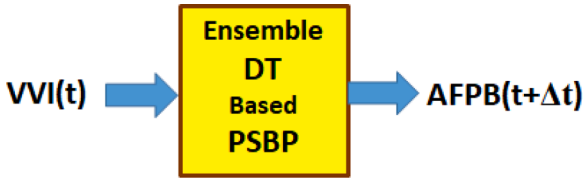

Fig. 5. Functional input/output of the PSBP.

classes of blackout (A, B, C), PSBP consists of two ensemble DTs with the functional structure shown in Table 3.

As it is shown in Table 3, ensemble DT1 is trained to discriminate between class A (1) and combined classes B+C (0), while, ensemble DT2 is trained to discriminate between combined classes A+B (1) and class C (0). The strategy for combining the output of each ensemble DT for reaching to final classification is shown in Table 4.

Table 3
Ensemble DTs for blackout areas.

Ensemble DT	Class ensemble 1 Output=1	Class ensemble 2 Output=0
Ensemble DT1	A	B+C
Ensemble DT2	A+B	C

Table 4
Combinatorial Ensemble DTs for predicting blackout classes.

Case	Ensemble DT1	Ensemble DT2	Class
Case1	1	1	A
Case2	0	1	B
Case3	0	0	C

Since the proposed predictor need only measured operating variables which are available in the control center so, it can easily be implemented in real time operation of power systems. By measuring system operating variables every one second and gathering them in control center, the moving window can be easily evaluated in the control center from which DDI can be incrementally and consecutively evaluated. Therefore, by presenting incremental change in MWS, DDI and VVI to ensemble DTs, the future potential blackout can be predicted. In fact, incremental learning is based on the measuring incremental change in operating condition presented by operating variables. The feasibility and usefulness of this method is based on two facts.

1. The behaviour of a power system is reflected in a moving window consisting of ns snapshots of transient operating variables from past to the present time t.

2. By using measured system operating variables at the control center every one second, the moving window of snapshots can be easily

evaluated in the control center from which DDI can be incrementally and consecutively evaluated. Thereafter, by presenting incremental change in MWS, DDI and VVI to the trained ensemble DT, the future potential blackout can be predicted.

4. Case study: IEEE 39-bus test system

The IEEE 39-bus test system with 10 generators and 34 lines is used to verify the capabilities of the proposed PSBP to predict the amount of potential blackout. Simulation of cascading failures (CFs) are performed using Power Factory@ software environment [40]. considering all components of a power system (generators, transformers, transmission lines, buses, loads and protection devices) with full dynamic characteristics. The goal of the simulation is to prepare the data set for offline training of the proposed PSBP.

4.1. Cascading failure simulation module

For preparing blackout trajectory, it is necessary to simulate cascading failure leading to blackout. For this purpose, using Power Factory@ software, a cascading failure simulation module (CFSM) is developed in which all generators and their controllers, such as automatic voltage regulators (AVRs) and governors (GOVs), are modeled. GAST turbine-governor model is considered for gas units and IEEE-G1 model is considered for thermal units [41]. The IEEE-DC1 model is used for generator exciters [42]. Protective relays including distance and over current relay for lines and transformers, out of step relay for generators, under frequency/voltage load shedding (UFLS) relays for loads, under voltage relays for lines, which are responsible for tripping transmission lines, transformers and generators during emergency conditions are modelled. UFLS relays have four frequency setting as 49.4, 49.2, 49 and 48.7 Hz with the corresponding load shed equal to 3.2 %, 6.7 %, 7.4 % and 8.7 %, respectively. Under voltage relay are set at voltage setting of 0.5 p.u. with tolerance period of 4s and delay of 0.01s. Overload relays for lines and transformers are set at 15s and 25s respectively. Turbine over/under speed trips are set at frequencies of 52 Hz and 47.7 Hz, respectively. All loads are modelled based on voltage and frequency dependency, and are connected to high voltage buses through load transformers equipped with tap changers and AVR. In fact, CFSM is capable to simulate the process of cascading following any disturbance in time domain until the system reaches to a new steady state operating point.

4.2. Training dataset

Training data required for training the proposed predictor PSBP are calculated using CFSM through several disturbance scenarios. For this purpose, 11 load levels, including 4200, 4500, 4800, 5100, 5400, 5700, 6000, 6300, 6600, 6900 and 7200 MW with their basic load-generation pattern, are adopted to obtain scenarios for cascading failure simulations. With respect to each basic load-generation pattern, using random variation in load-generation defined by Eqs (6) and (7), nine additional load-generation patterns are generated. Totally, 110 load-generation patterns are produced.

$$PD_i^L = PD_i^1 + 300(1+\alpha_i)(L-1) \quad \forall L = 2, \ldots, 11 \quad , \quad -0.5 < \alpha_i < +0.5 \tag{6}$$

$$PG_i^L = PG_i^1 + 300(1+\beta_i)(L-1) \quad \forall L = 2, \ldots, 11 \quad , \quad -0.5 < \beta_i < +0.5 \tag{7}$$

where PD_i^1, PG_i^1 are the initial load and generation at bus i, and the initial load level is 4200 MW and L refers to load level. For each load level, the zero value of α and β, refers to the basic load-generation pattern. In the light load condition, 1 to 3 generators are randomly taken out. The effects of changes in the network topology due to maintenance are considered in the training data. For this purpose, 1 to 3 lines due to maintenance are randomly taken out of the network. Basic topology and topology changes are considered for 110 load-generation patterns and their power flow is calculated resulted in 166 acceptable initial steady-state operating points. A list of 64 types of initial disturbances including a three-phase short-circuit fault at one line, a three-phase fault at one line simultaneous with the outage of another line close to the faulty bus, and complete outages of all lines connected to a bus is prepared. Each of the 166 steady-state operating points is disturbed by one of the initial disturbances, which results in different scenarios with mild to severe conditions. The number of all disturbed scenarios is equal to 1000, which are simulated by CFSM in the time domain for 240 seconds. With respect to all scenarios, 1000 PSBT and BT are obtained with 1 second sampling time from which corresponding DTOVs, DDIs, CDDI, and VVIs are calculated.

The bus voltage magnitude (V), phase angle (θ), line current magnitude (I) and bus frequency (f) of each BA constitute corresponding DTOV for that area. The amount of blackout on BT for each BA constitutes AFPB. The length of MWS is 10 seconds including 11 snapshots with associated DTOVs.

In this paper, the predicting time for AFPB(t+Δt), is considered as Δt=5 s, and it means that each MWS(t) can predict its respective AFPB 5 seconds ahead. Blackout prediction of 5 seconds ahead is justified because it gives a delay sufficient for tripping various relays.

Then, there are a number of 230Nb samples of CDDIs(t) and their AFPBs(t+5) for Nb blackout areas per disturbed operating point scenario, and totally a number of 230000Nb samples of CDDIs(t) and their respective AFPBs (t +5) for Nb blackout areas for 1000 disturbed operating point scenarios. Finally, by using the MI method instead of the CDDI(t) vector including 48 DDIs, the dominant CDDIs are identified as the final vector for constructing the VVI. It should be mentioned that the VVI is different for each ensemble DT in each BA. In other words, 2 distinct VVI are provided for each BA and a total of 2Nb distinct VVI are provided for all Nb blackout areas.

4.3. Blackout area identification

For identification BA, Jaccard indices are first evaluated for all loads through 1000 disturbance-scenarios. Fig. 6 shows the number of times that each of the 19 loads is isolated from the network separately in the 700 training scenarios. For example, loads No. 7 and 8 are isolated in 268 and 253 out of 700 scenarios respectively. Fig. 7 shows the number of times that load 7 is isolated simultaneously with other loads within a 15s-interval. For example, the simultaneous isolation of loads No. 7 and 8 occurs in 201 out of 700 scenarios.

Regarding the values on Figs. 5 and 6, according to (1), the value of the Jaccard measure for loads 7 and 8 is evaluated as follows:

$$Jaccard_{7-8} = \frac{C_{7-8}}{A_7 + B_8 - C_{7-8}} = \frac{201}{268 + 253 - 201} = 0.628$$

After acquiring the values of the Jaccard indices for all pairs of loads and running the algorithm in Section (2.1), all loads are categorized in 6 BAs as shown in Fig. 8. Bus No. 39 constitutes one area because the isolation of its load has less correlation with other loads, and its Jaccard index shows a very low probability of simultaneous isolation with other loads.

4.4. Dominant transient operating variables (DTOVs) of lines and busbars

After identifying BAs, according to the algorithm of Section 2.2 for each BA, the Jaccard indices of all loads with all lines and busbars are evaluated. The lines or busbars with Jaccard index higher than a threshold value ε ($\varepsilon = Average + STDEV$) are recognized as elements

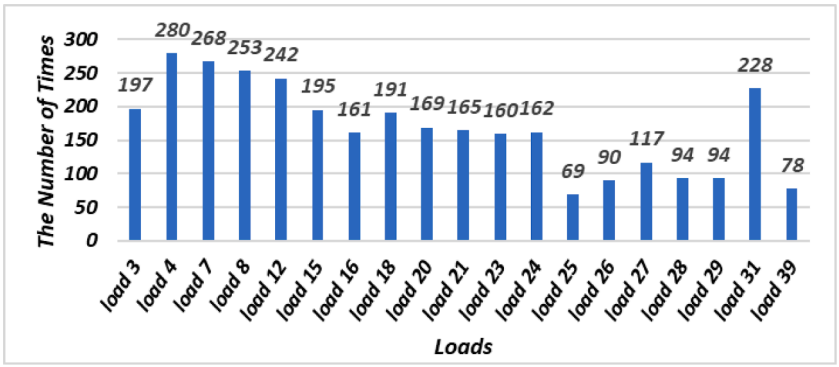

Fig. 6. Number of isolations of each load from test system.

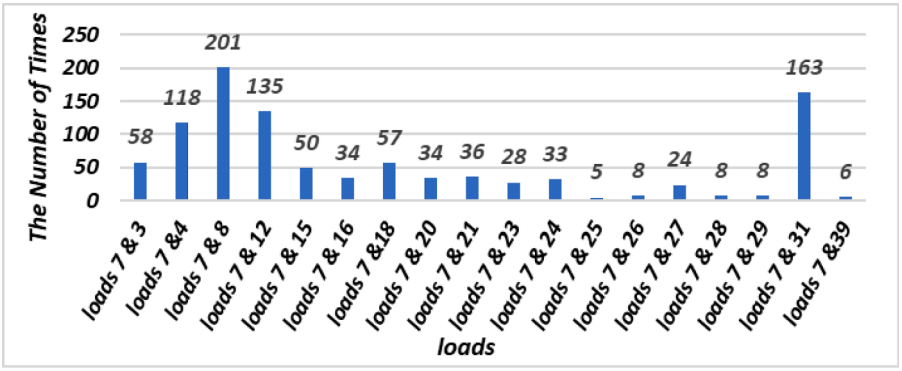

Fig. 7. Number of simultaneous isolations of load 7 with other loads.

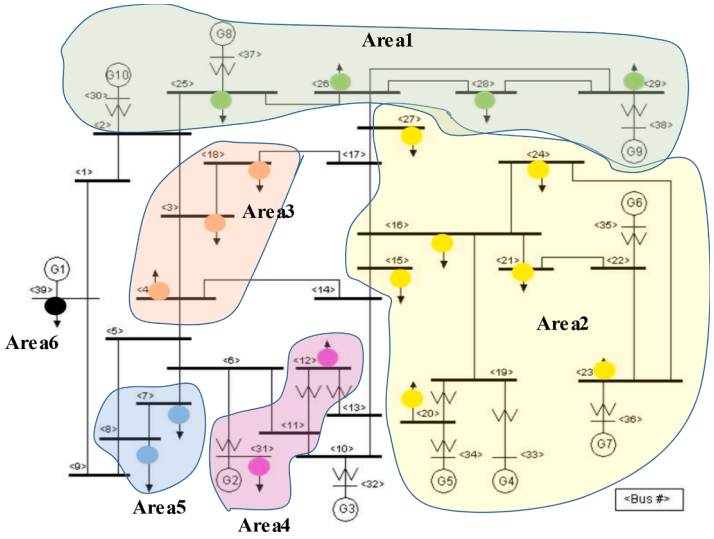

Fig. 8. Areal blackouts in IEEE 39-bus test system.

whose operating variables constitutes DTOV. The threshold value ε for each BA is determined based on the average of the Jaccard indices of all lines and busbars with loads of that BA. Loads 7 and 8 are in area 5, and Fig. 9 shows their Jaccard indices with all network lines. As can be seen only 6 lines have indices greater than average which constitutes DTOV of area 5. Table 5 reports the lines and busbars having the dominant variables for each BA in the IEEE 39-bus test system.

4.5. Areal blackout classes

With respect to all 1000 disturbed scenarios, 230,000 VVIs(t) are obtained from which 161,000 (70 %) and 69,000 (30 %) are selected for training and test respectively. By calculating the Ward distance Wdij between VVIs of all pairs (i, j) of the training data, and using hierarchical clustering (HC) algorithm, three blackout classes are recognized. Table 6 shows the number of VVIs(t) of each blackout class and their corresponding AFPB for 6 BAs. According to this Table, the three blackout classes A, B and C show low, moderate and critical conditions,

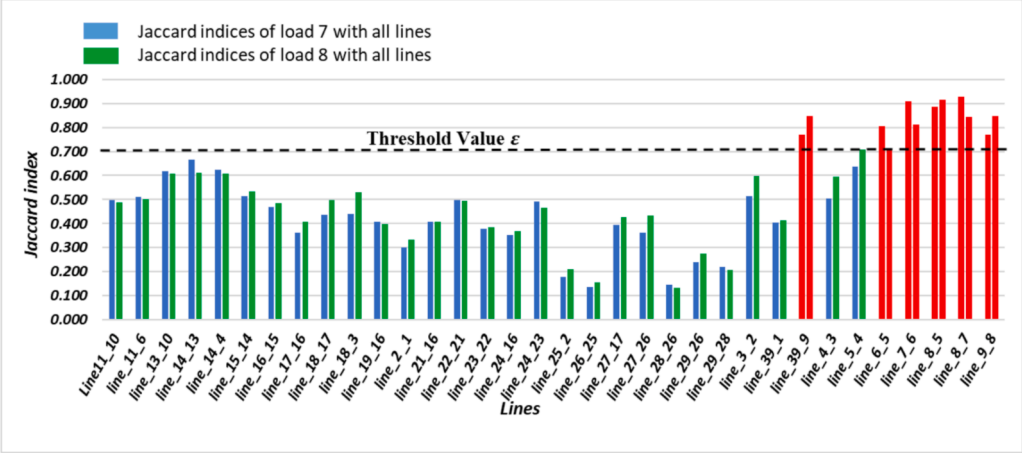

Fig. 9. Jaccard indices of loads 7 and 8 with all lines.

Table 5
Lines and busbars having dominant areal variables in blackout areas.

Area	Type	Line number or busbar
Area1	Lines	2–1, 25–2, 26–25, 28–26, 29–26, 29–28
	Busbars	2, 25, 26, 28, 29, 30, 37, 38
Area2	Lines	15–14, 16–15, 19–16, 21–16, 22–21, 23–22, 24–16, 24–23, 27–17, 27–26
	Busbars	15, 16, 17, 19, 20, 21, 22, 23, 24, 26, 27, 33, 34, 35, 36
Area3	Lines	15_14, 18_17, 18_3, 21_16, 22_21, 24_23, 27_17, 27_26, 3_2
	Busbars	2, 3, 4, 16, 18, 21, 24, 27, 30, 39
Area4	Lines	11–10, 11–6, 13–10, 14–13, 15–14, 16–15, 22–21, 24–23, 6–5, 7–6
	Busbars	6, 11, 12, 13, 31
Area5	Lines	39–9, 6–5, 7–6, 8–5, 8–7, 9–8
	Busbars	5, 6, 7, 8, 9, 31
Area6	Lines	2–1, 39–1
	Busbars	30, 39

Table 6
Areal blackout (%) classes and number of VVIs(t).

Aea	Class	Number of VVIs(t)	Range of AFPB
Area 1	Class A	149,410 (92.8%)	0% - 34.1%
	Class B	5323 (3.3%)	34.1 % - 74.6%
	Class C	6267 (3.9%)	74.6% - 100%
Area 2	Class A	128,923 (80.1%)	0% - 23.6%
	Class B	8848 (5.5%)	23.6 % - 80.3%
	Class C	23,229 (14.4%)	80.3% - 100%
Area 3	Class A	108,682 (67.5%)	0% - 44.6%
	Class B	16,694 (10.4%)	44.6 % - 55.2%
	Class C	35,624 (22.1%)	55.2% - 100%
Area 4	Class A	117,251 (72.8%)	0% - 88.2%
	Class B	4119 (2.6%)	88.2 % - 95.9%
	Class C	39,630 (24.6%)	95.9% - 100%
Area 5	Class A	107,734 (66.9%)	0% - 30.7%
	Class B	6819 (4.2%)	30.7 % - 77.6%
	Class C	46,447 (28.8%)	77.6% - 100%
Area 6	Class A	152,604 (94.8%)	0% - 26.6%
	Class B	2096 (1.3%)	26.6% - 83.1%
	Class C	6300 (3.9%)	83.1% - 100%

respectively.

According to Table 6, blackout ranges in all three classes are different from each other in the 6 BAs. The structure of BAs of the power systems is the reason for such a difference.

4.6. Power system blackout predictor (PSBP)

Each BA has its own PSBP which is a combination of ensemble DTs in which categorization between three classes can be obtained by two ensemble DTs. Table 3 shows the logical structure of the proposed PSBP. For the ensemble DT, there are five types including Bag, GentleBoost, LogitBoost, RUSBoost and AdaBoosM1 algorithms [43]. By using Bayesian optimization and 10-fold validation [44], the predictor parameters are designed and the ensemble learning algorithms are selected. The PSBP of each BA consists of two ensemble DTs with the corresponding VVI which are determined based on MI index as shown in Table 7. For example, $CDDI4_F$ stands for CDDI4 related to the busbar frequency signal. Each ensemble DTs is trained using its respective VVI.

Table 8 shows the results of the training for ensemble DTs of 6 BAs.

As shown in Table 8, the number of times that the AdaboostM1 is selected as training algorithm is more than other learning algorithms indicating the superior performance of this algorithm for this case study.

Table 7
Areal ensemble DTs with respective CDDIs and VVIs.

Area	Ensemble DT	Dominant CDDIs constituting VVI	Size of VVI
Area1	Ensemble DT1	$CDDI2_\Theta$, $CDDI2_V$, $CDDI3_\Theta$, $CDDI3_V$, $CDDI4_F$, $CDDI5_V$, $CDDI8_F$, $CDDI8_V$, $CDDI10_V$, $CDDI11_V$	10
	Ensemble DT2	$CDDI1_V$, $CDDI4_V$, $CDDI5_V$, $CDDI11_F$	4
Area2	Ensemble DT1	$CDDI7_I$, $CDDI7_F$, $CDDI7_V$, $CDDI9_I$, $CDDI12_I$, $CDDI12_F$	6
	Ensemble DT2	$CDDI3_V$, $CDDI4_V$, $CDDI5_F$, $CDDI8_V$, $CDDI10_V$, $CDDI11_V$	6
Area3	Ensemble DT1	$CDDI3_V$, $CDDI5_V$, $CDDI10_V$	3
	Ensemble DT2	$CDDI1_F$, $CDDI1_\Theta$, $CDDI1_V$, $CDDI2_F$, $CDDI2_\Theta$, $CDDI2_V$, $CDDI6_\Theta$, $CDDI11_F$, $CDDI12_\Theta$	9
Area4	Ensemble DT1	$CDDI4_V$, $CDDI6_V$	2
	Ensemble DT2	$CDDI2_\Theta$, $CDDI3_F$, $CDDI3_\Theta$, $CDDI3_V$, $CDDI4_F$, $CDDI4_V$, $CDDI5_F$, $CDDI5_V$, $CDDI6_V$, $CDDI8_F$, $CDDI8_V$, $CDDI10_F$, $CDDI10_\Theta$, $CDDI10_V$, $CDDI11_V$	15
Area5	Ensemble DT1	$CDDI7_I$, $CDDI7_F$, $CDDI7_V$, $CDDI9_I$, $CDDI12_I$, $CDDI12_F$, $CDDI12_V$	7
	Ensemble DT2	$CDDI3_\Theta$, $CDDI3_V$, $CDDI8_V$, $CDDI10_\Theta$	4
Area6	Ensemble DT1	$CDDI1_F$, $CDDI2_F$, $CDDI3_F$, $CDDI4_F$, $CDDI5_F$, $CDDI6_F$, $CDDI11_F$	7
	Ensemble DT2	$CDDI1_\Theta$, $CDDI1_V$, $CDDI2_\Theta$, $CDDI2_V$, $CDDI3_\Theta$, $CDDI3_V$, $CDDI4_V$, $CDDI5_V$, $CDDI6_V$, $CDDI8_V$, $CDDI10_\Theta$, $CDDI10_V$, $CDDI11_V$	13

Table 8
Training result for 12 ensemble DTs in 6 BAs.

Area	Characteristics						
	Ensemble DT	Ensemble learning algorithm	Number of ensemble learning cycles	Learning rate for shrinkage	Split criterion	Maximal number of decision splits	Minimum number of leaf node observations
Area 1	Ensemble DT1	AdaBoostM1	496	0.033253	deviance	122,240	12
	Ensemble DT2	Bag	11	NaN	deviance	41,229	3
Area 2	Ensemble DT1	AdaBoostM1	10	0.001514	gdi	139,850	2
	Ensemble DT2	AdaBoostM1	439	0.24755	gdi	104,240	4
Area 3	Ensemble DT1	AdaBoostM1	10	0.7206	deviance	38	2
	Ensemble DT2	AdaBoostM1	10	0.92437	gdi	52,400	1
Area 4	Ensemble DT1	RUSBoost	26	0.22065	gdi	82	4
	Ensemble DT2	AdaBoostM1	205	0.52057	deviance	146,070	17
Area 5	Ensemble DT1	AdaBoostM1	26	0.74952	deviance	2645	1
	Ensemble DT2	Bag	88	NaN	gdi	21,752	5
Area 6	Ensemble DT1	GentleBoost	262	0.30878	undefined	5	1988
	Ensemble DT2	RUSBoost	23	0.90426	gdi	71	5

5. Discussion

5.1. Training Results

The training result in (Tables 9,10,11,12,13,14) show that the training performance of the proposed predictors are different for blackout areas. The best performance is obtained for areas BA1 and BA2 consisting of 4 and 6 load buses, with respect to all classes. While the lowest accuracy is obtained for area 4 and 6 consisting of 2 and 1 load buses respectively. Comparing the accuracy of areas, it can be concluded that as the number of load buses decreases in an area the accuracy of its predictor decreases and this is due to discrete behavior of loads during blackout which makes training hard. Because the load variation due to blackout in an area with bigger number of load buses is more continuous compared to the area with lower number of load buses. This characteristic can be regarded as an additional criterion for selecting the proper size of blackout area. Another point which can be understood is that the average accuracy of the proposed predictor for classes A, B and C are 99.86, 95.50 and 98.47 respectively which are in a close correlation with the total number of training data for these classes which are 736,715, 42,807 and 155,281 respectively. It means that the number of data could affect training performance and in another words for each class sufficient training data should be prepared.

5.2. Validation of PSBP performance

The predictive performance of the trained PSBP is evaluated using

Table 9
Training accuracy of PSBP in term of DTs performance in BA1.

Predicted Actual	Class A (1, 1)	Class B (1, 0)	Class C (0, 0)	Without Class (0, 1)
Class A	**149,408 (99.99%)**	**0 (0%)**	**0 (0%)**	**2 (0.001%)**
Class B	**0 (0%)**	**5321 (99.96%)**	**2 (0.04%)**	**0 (0%)**
Class C	**0 (0%)**	**75 (1.2%)**	**6192 (98.80%)**	**0 (0%)**

Table 10
Training accuracy of PSBP in term of DTs performance in BA2.

Predicted Actual	Class A (1, 1)	Class B (1, 0)	Class C (0, 0)	Without Class (0, 1)
Class A	**128,787 (99.89%)**	**136 (0.11%)**	**0 (0%)**	**0 (0%)**
Class B	**69 (0.78%)**	**8779 (99.22%)**	**0 (0%)**	**0 (0%)**
Class C	**0 (0%)**	**0 (0%)**	**23,207 (99.9%)**	**22 (0.1%)**

Table 11
Training accuracy of PSBP in term of DTs performance in BA3.

Predicted Actual	Class A (1, 1)	Class B (1, 0)	Class C (0, 0)	Without Class (0, 1)
Class A	**108,328 (99.67%)**	**354 (0.33%)**	**0 (0%)**	**0 (0%)**
Class B	**333 (1.99%)**	**16,361 (98.01%)**	**0 (0%)**	**0 (0%)**
Class C	**0 (0%)**	**0 (0%)**	**35,124 (98.60%)**	**500 (1.40%)**

Table 12
Training accuracy of PSBP in term of DTs performance in BA4.

Predicted Actual	Class A (1, 1)	Class B (1, 0)	Class C (0, 0)	Without Class (0, 1)
Class A	**117,165 (99.93%)**	**86 (0.07%)**	**0 (0%)**	**0 (0%)**
Class B	**192 (4.66%)**	**3927 (95.34%)**	**0 (0%)**	**0 (0%)**
Class C	**0 (0%)**	**0 (0%)**	**38,867 (98.07%)**	**763 (1.93%)**

Table 13
Training accuracy of PSBP in term of DTs performance in BA5.

Predicted Actual	Class A (1, 1)	Class B (1, 0)	Class C (0, 0)	Without Class (0, 1)
Class A	**107,710 (99.98%)**	**0 (0%)**	**0 (0%)**	**24 (0.02%)**
Class B	**0 (0%)**	**6693 (98.15%)**	**126 (1.85%)**	**0 (0%)**
Class C	**0 (0%)**	**468 (1.01%)**	**45,861 (98.74%)**	**118 (0.25%)**

Table 14
Training accuracy of PSBP in term of DTs performance in BA6.

Predicted Actual	Class A (1, 1)	Class B (1, 0)	Class C (0, 0)	Without Class (0, 1)
Class A	**152,317 (99.81%)**	**248 (0.16%)**	**16 (0.01%)**	**23 (0.02%)**
Class B	**348 (16.6%)**	**1726 (82.35%)**	**8 (0.38%)**	**14 (0.67%)**
Class C	**17 (0.27%)**	**30 (0.48%)**	**6093 (96.71%)**	**160 (2.54%)**

Table 15
PSBP accuracy under test mode for blackout areas.

Class Area	Class A	Class B	Class C	Overall Accuracy
Area 1	**63,284 (99.9%)**	**2368 (96.1%)**	3069 (96.3%)	**68,721 (99.6%)**
Area 2	**49,673 (97.3%)**	**4706 (88.9%)**	**12,339 (97.6%)**	**66,718 (96.7%)**
Area 3	**41,042 (96.1%)**	**7711 (93.1%)**	**17,207 (95.5%)**	**65,960 (95.6%)**
Area 4	**46,125 (99.3%)**	**1911 (95.8%)**	**20,097 (97.7%)**	**68,133 (98.7%)**
Area 5	**39,812 (99.1%)**	**3391 (83.7%)**	**23,900 (96.5%)**	**67,103 (97.3%)**
Area 6	**65,147 (99.8%)**	**661 (83.1%)**	**2792 (96.1%)**	**68,600 (99.4%)**

69,000 unseen cases for each BA as shown in Table 15. The results show that the proposed PSBP has a good predicting output nearly similar to training results which validate its performance. The overall weighted prediction accuracy for classes A, B and C within 6 areas are 98.84, 90.88 and 96.75 respectively which are in accordance with the accuracy of the training performance for those classes. The reason for low accuracy of predictor of class B compared to classes A and C is due to the lack of sufficient training data and low training accuracy. Again at the test stage, this fact that for each class, sufficient training data should be prepared is emphasized. In order to show the test performance of the predictors for 3 classes in 6 areas, with respect to 69,000 test data, the overall performance of each PSBP is evaluated by more performance indices including the overall accuracy (OAC), sensitivity (SEN), specificity (SP) and balanced accuracy (BAC) [45] for 6 areas using Eqs. (8–11) as shown in Fig. 10. As it is seen, all indices support training performance of the predictors and the balance accuracy is in accordance with the overall accuracy.

$$OACi = \frac{TN_i + TP_i}{TP_i + TN_i + FP_i + FN_i} \forall\, i = 1, \ldots, 6 \tag{8}$$

$$SENi = \frac{TP_i}{TP_i + FN_i} \forall\, i = 1, \ldots, 6 \tag{9}$$

$$SPi = \frac{TN_i}{TN_i + FP_i} \forall\, i = 1, \ldots, 6 \tag{10}$$

$$BACi = \frac{SENi + SPi}{2} \forall\, i = 1, \ldots, 6 \tag{11}$$

5.3. Robustness of PSBP

The noisy and missed data are two factors affecting the performance of the proposed PSBP. For this purpose, the robustness of PSBP with respect to noisy and missed data are evaluated. For noisy data, based on C37.118.2–2011 IEEE standard, random noisy data with the maximum value of 1 % are added to the measurement data of DTOV [46]. The reason for missed data are PMU malfunction, telecommunication system and cyber-attack [13]. For missed data, 20 % of variables of DTOVs are randomly selected and lost. Using DTOV with noisy and missed data, all steps of data processing for evaluating corresponding VVI are carried out for three cases; Case 1 with only noisy data, case 2 with only missed data and case 3 with both noisy and missed data. Fig. 11 shows the performance of PSBP in term of BAC for three cases. As it can be seen, the noisy and missing data have little impact on the accuracy of the PSBP for all 6 BAs. The reason for the decrease in the accuracy in the area 5 is that adding noisy or missed data cause overlapping of the classes belonging to that area.

6. Conclusion

This paper presents a paradigm shift in vulnerability assessment, where the future behavior of a power system towards blackouts under emergency conditions is predicted based on its current and historical behavior. The causal relationship between the historical behavior of power systems and the potential future blackouts serves as the foundation for this innovative approach. This approach serves as a supplementary tool to compensate for the limitations of conventional DSA methods in preventing blackouts. It is shown that for enhancing prediction accuracy and practical applicability, based on the historical behavior of load buses during blackout experiences, the whole power network is better to be divided into several blackout-prone areas where for each area, a dedicated predictor is designed. A new sophisticated vulnerability indices are introduced which are derived from raw

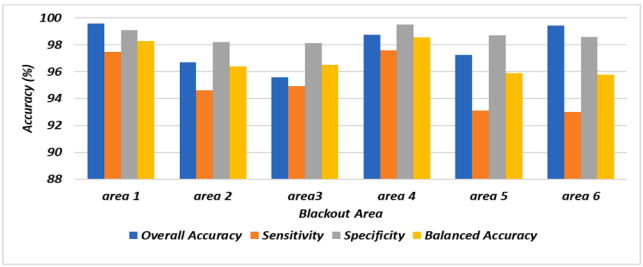

Fig. 10. Overall performance of PSBP for the 6 areal blackouts.

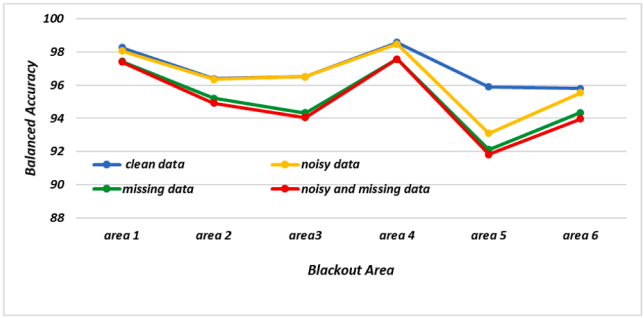

Fig. 11. Performance of PSBP against simultaneous noisy and missing data.

operational data and independent from network-size and configuration and can effectively capture the trend of system vulnerability. The most interesting achievement for this paper is demonstrating this fact that just relying on transient operating data without any need to additional data like system parameter, configuration, disturbance and controllers, is sufficient for vulnerability assessment in future time ahead. The training results show that the number of load buses within each blackout area can affect the training performance of its predictor. Because an area with a little number of load buses has a discrete load behavior during blackout which reduces the training performance. Also it is shown that low training data specifically for the most critical condition represent by classes B and C, can affect their prediction performance. The proposed vulnerability indices show acceptable robustness against missing data and broad noise without any need to data substitution, model observability, or PMU observability, by solely relying on dominant transient operating variables. Simulation results show that the overall noisy and missing data have little impact of 1–4% on the blackout predictor accuracy in blackout areas. The proposed predictor can be used as an alarming tool for arming emergency corrective action under emergency conditions.

CRediT authorship contribution statement

Siavash Shadpey: Writing – original draft, Validation, Software, Methodology, Formal analysis. **Mohammad Reza Aghamohammadi:** Writing – review & editing, Supervision, Project administration, Conceptualization. **Alireza Sobbouhi:** Writing – review & editing, Visualization, Supervision, Conceptualization. **Enrico Zio:** Writing – review & editing, Visualization.

Declaration of competing interest

The authors declare that they have no known competing financial interests or personal relationships that could have appeared to influence the work reported in this paper.

Data availability

Data will be made available on request.

References

[1] T.E. Dy Liacco, Systems security: The computer's role, IEEE Spectr. 15 (1978) 43–50.

[2] A. Varbella, B. Gjorgiev, G. Sansavini, Geometric deep learning for online prediction of cascading failures in power grids, Reliab. Eng. Syst. Saf. 237 (2023) 109341.

[3] C. Ren, H. Yu, Y. Xu, Z.Y. Dong, Understanding discrepancy of power system dynamic security assessment with unknown faults: A reliable transfer learning-based method, CSEE J. Power and Energy Systems 10 (1) (2024) 427–431. January.

[4] L. Zhu, et al., Robust representation learning for power system short-term voltage stability assessment under diverse data loss conditions, In IEEE Trans. Neural Netw. Learn. Syst. 35 (5) (2024) 6035–6047. May.

[5] Z. Li, J Yan, Y Liu, W Liu, L Li, H Qu, Power system transient voltage vulnerability assessment based on knowledge visualization of CNN, Int. J. Electr. Power Energy Syst. 155 (2024) 109576.

[6] M. Abedi, M.R. Aghamohammadi, M.T. Ameli, SVM based intelligent predictor for identifying critical lines with potential for cascading failures using pre-outage operating data, Int. J. Electr. Power Energy Syst. 136 (2022) 107608.

[7] Y. Lin, X. Wang, A data-driven scheme based on sparse projection oblique randomer forests for real-time dynamic security assessment, IEEe Access. 10 (2022) 79469–79479.

[8] C. Ren, H. Yuan, Q. Li, R. Zhang, Y. Xu, Pre-fault dynamic security assessment of power systems for multiple different faults via multi-label learning, IEEE Trans. Power Syst. 38 (6) (2023) 5501–5511. Nov.

[9] C. Ren, Y. Xu, B. Dai, R. Zhang, An integrated transfer learning method for power system dynamic security assessment of unlearned faults with missing data, IEEE Trans. Power Syst. 36 (5) (2021) 4856–4859. Sept.

[10] C. Li, Y. Liu, Online dynamic security assessment of wind integrated power system using SDAE with SVM ensemble boosting learner, Int. J. Electr. Power Energy Syst. 125 (2021) 106429.

[11] S. Liu, L. Liu, N. Yang, D. Mao, L. Zhang, J. Cheng, T. Xue, et al., A data-driven approach for online dynamic security assessment with spatial-temporal dynamic visualization using random bits forest, Int. J. Electr. Power Energy Syst. 124 (2021) 106316.

[12] T. Liu, et al., A bayesian learning based scheme for online dynamic security assessment and preventive control, IEEE Trans. Power Syst. 35 (5) (Sept. 2020) 4088–4099.

[13] C. Ren, Y. Xu, A fully data-driven method based on generative adversarial networks for power system dynamic security assessment with missing data, IEEE Trans. Power Syst. 34 (6) (2019) 5044–5052. Nov.

[14] Y. Zhang, Y. Xu, S. Bu, Z.Y. Dong, R. Zhang, Online power system dynamic security assessment with incomplete PMU measurements: A robust white-box model, IET Gener. Transm. Distrib. 13 (2019) 662–668, 5.

[15] C. Ren, Y. Xu, Transfer learning-based power system online dynamic security assessment: using one model to assess many unlearned faults, IEEE Trans. Power Syst. 35 (1) (2020) 821–824. Jan.

[16] Q. Li, Y. Xu, C. Ren, J. Zhao, A hybrid data-driven method for online power system dynamic security assessment with incomplete PMU Measurements, 2019, IEEE Power & Energy Society General Meeting (PESGM) (2019) 1–5. Atlanta, GA, USA.

[17] G.A. Nakas, A. Dirik, P.N. Papadopoulos, A.R.R. Matavalam, O. Paul, D. Tzelepis, Online identification of cascading events in power systems with renewable generation using measurement data and machine learning, IEEE Access. 11 (2023) 72343–72356.

[18] S. Jafarzadeh, V.M.I. Genc, Real-time transient stability prediction of power systems based on the energy of signals obtained from PMUs, Electr. Power Syst. Res. 192 (2021) 107005.

[19] M. Zhang, J. Li, Y. Li, R. Xu, Deep learning for short-term voltage stability assessment of power systems, IEEE Access. 9 (2021) 29711–29718.

[20] K. Ding, Y. Qian, Y. Wang, P. Hu, B. Wang, A data-driven vulnerability evaluation method in grid edge based on random matrix theory indicators, IEEE Access. 8 (2020) 26495–26504.

[21] Z. Shi, W. Yao, L. Zeng, J. Wen, J. Fang, X. Ai, J. Wen, Convolutional neural network-based power system transient stability assessment and instability mode prediction, Appl. Energy 263 (2020) 114586.

[22] B. Tan, J. Yang, T. Zhou, X. Zhan, Y. Liu, S. Jiang, C. Luo, Spatial-temporal adaptive transient stability assessment for power system under missing data, Int. J. Electr. Power Energy Syst. 123 (2020) 106237.

[23] M.R. Aghamohammadi, M. Abedi, DT based intelligent predictor for out of step condition of generator by using PMU data, Int. J. Electr. Power Energy Syst. 99 (2018) 95–106.

[24] M.R. Salimian, M.R. Aghamohammadi, A three stages decision tree-based intelligent blackout predictor for power systems using brittleness indices, IEEe Trans. Smart. Grid. 9 (5) (2018) 5123–5131. Sept.

[25] Y. Zhang, Y. Xu, R. Zhang, Z.Y. Dong, A missing-data tolerant method for data-driven short-term voltage stability assessment of power systems, IEEe Trans. Smart. Grid. 10 (5) (2019) 5663–5674. Sept.

[26] J.C. Cepeda, J.L. Rueda, D.G. Colomé, I. Erlich, Data-mining-based approach for predicting the power system post-contingency dynamic vulnerability status, Int. Trans. Electr. Energy Syst. 25 (2015) 2515–2546, 10.

[27] G. Fotis, V. Vita, T.I. Maris, Risks in the European transmission system and a novel restoration strategy for a power system after a major blackout, Appl. Sci. 13 (1) (2022) 83.

[28] V. Vita, G. Fotis, C. Pavlatos, V. Mladenov, A new restoration strategy in microgrids after a blackout with priority in critical loads, Sustain. 15 (3) (2023) 1974.

[29] S. Deb, S. Lata, V.S. Bhadoria, S. Tiwari, T.I. Maris, V. Vita, G. Fotis, Improved relay algorithm for detection and classification of transmission line faults in monopolar HVDC transmission system using signum function of transient energy, IEEe Access. (2024).

[30] H. Finch, Comparison of distance measures in cluster analysis with dichotomous data, J. Data Sci. 3 (1) (2005) 85–100.

[31] D. Pfitzner, R. Leibbrandt, D. Powers, Characterization and evaluation of similarity measures for pairs of clusterings, Knowl. Inf. Syst. 19 (2009) 361–394.

[32] S.T. Wierzchoń, M.A. Kłopotek, Modern algorithms of cluster analysis, Springer International Publishing, 2018. Vol. 34.

[33] D.J. Weller-Fahy, B.J. Borghetti, A.A. Sodemann, A survey of distance and similarity measures used within network intrusion anomaly detection, In IEEE Commun. Surv. Tutor. 17 (1) (2015) 70–91. Firstquarter.

[34] E.F. Krause, Taxicab geometry: An adventure in non-Euclidean geometry, Courier Corporation, 1986.

[35] A.G. Asuero, A. Sayago, A.G. González, The correlation coefficient: An overview, Crit. Rev. Anal. Chem. 36 (1) (2006) 41–59.

[36] V. Monev, Introduction to similarity searching in chemistry, MATCH Commun. Math. Comput. Chem 51 (2004) 7–38.

[37] R. Battiti, Using mutual information for selecting features in supervised neural net learning, IEEe Trans. Neural Netw. 5 (4) (1994) 537–550. July.

[38] F. Murtagh, P. Contreras, Algorithms for hierarchical clustering: an overview, II, Wiley Interdiscip. Rev.: Data Min. Knowl. Discov. 7 (6) (2017) e1219.

[39] L. Yang, M. Aghaabbasi, A. Mujahid, A. Jan, B. Bouallegue, M.F Javed, N.M. Salem, Comparative analysis of the optimized KNN, SVM, and ensemble DT models using Bayesian optimization for predicting pedestrian fatalities: an advance towards realizing the sustainable safety of pedestrians, Sustain. 14 (17) (2022) 10467.

[40] F.M. Gonzalez-Longatt, J.L. Rueda, PowerFactory applications for power system analysis, Springer, 2014.

[41] P. Pourbeik, Dynamic models for turbine-governors in power system studies, IEEE Task Force on TurbineGovernor Modeling (2013).

[42] D.C. Lee, IEEE recommended practice for excitation system models for power system stability studies (IEEE Std 421.5-1992), Energy Development and Power Generating Committee of the Power Engineering Society (1992).
[43] Z.H. Zhou, Ensemble methods: foundations and algorithms, CRC press, 2012.
[44] M.A. Awal, M. Masud, M.S. Hossain, A.A.M. Bulbul, S.M. Hasan Mahmud, A. K. Bairagi, A novel bayesian optimization-based machine learning framework for COVID-19 detection from inpatient facility data, IEEe Access. 9 (2021) 10263–10281.
[45] K.H. Brodersen, C.S. Ong, K.E. Stephan and J.M. Buhmann, "The balanced accuracy and its posterior distribution", 2010 20th International Conference on Pattern Recognition, Istanbul, Turkey, 2010, pp. 3121–3124.
[46] M. He, V. Vittal, J. Zhang, Online dynamic security assessment with missing PMU measurements: A data mining approach, IEEE Trans. Power Syst. 28 (2) (2013) 1969–1977.